



Published in final edited form as:

*Leukemia*. 2019 October ; 33(10): 2429–2441. doi:10.1038/s41375-019-0454-4.

## Transient stabilization, rather than inhibition of MYC amplifies extrinsic apoptosis and therapeutic responses in refractory B-cell lymphoma

Colleen T. Harrington<sup>1,7,\*</sup>, Elena Sotillo<sup>1,&,\*</sup>, Aude Robert<sup>10</sup>, Katharina E. Hayer<sup>3</sup>, Agata M. Bogusz<sup>4</sup>, James Psathas<sup>1,\$</sup>, Duonan Yu<sup>1,#</sup>, Deanne Taylor<sup>3,5</sup>, Chi V. Dang<sup>8</sup>, Peter Klein<sup>6,7</sup>, Michael D. Hogarty<sup>2,5,7</sup>, Birgit Geoerger<sup>11,12</sup>, Wafik S. El-Deiry<sup>9</sup>, Joëlle Wiels<sup>10</sup>, Andrei Thomas-Tikhonenko<sup>1,2,4</sup>

<sup>1</sup>Division of Cancer Pathobiology, Children's Hospital of Philadelphia; Philadelphia, PA 19104

<sup>2</sup>Division of Oncology, Children's Hospital of Philadelphia; Philadelphia, PA 19104

<sup>3</sup>Division of Bioinformatics Group, Children's Hospital of Philadelphia; Philadelphia, PA 19104

<sup>4</sup>Department of Pathology and Laboratory Medicine, Perelman School of Medicine at the University of Pennsylvania, Philadelphia, PA 19104

<sup>5</sup>Department of Pediatrics, Perelman School of Medicine at the University of Pennsylvania, Philadelphia, PA 19104

<sup>6</sup>Department of Medicine, Perelman School of Medicine at the University of Pennsylvania, Philadelphia, PA 19104

<sup>7</sup>Department of Cell & Molecular Biology Graduate Group, Perelman School of Medicine at the University of Pennsylvania, Philadelphia, PA 19104

<sup>8</sup>Molecular and Cellular Oncogenesis Program, The Wistar Institute, Philadelphia, PA 19104

<sup>9</sup>Pathology and Laboratory Medicine, Brown University Medical School, Providence, RI 02912

<sup>10</sup>CNRS UMR 8126, Univ Paris-Sud - Université Paris-Saclay, Institut Gustave Roussy, 94805 Villejuif, France

<sup>11</sup>CNRS UMR 8203, Univ Paris-Sud - Université Paris-Saclay, Institut Gustave Roussy, 94805 Villejuif, France

<sup>12</sup>Department of Pediatric and Adolescent Oncology, Univ Paris-Sud - Université Paris-Saclay, Institut Gustave Roussy, 94805 Villejuif, France

**Corresponding author:** Andrei Thomas-Tikhonenko, Ph.D., Children's Hospital of Philadelphia, 4056 Colket Translational Research Bldg, 3501 Civic Center Blvd, Philadelphia, PA 19104, Phone: 267-426-9699, Fax: 267-426-8125, andreit@pennmedicine.upenn.edu.

\*equal contribution

&present address: Stanford Cancer Institute, 265 Campus Dr., Stanford, CA 94305

#present address: Noncoding RNA Center, Yangzhou University, Yangzhou 225001, China

\$present address: The Janssen Pharmaceutical Companies of Johnson & Johnson, 200 Great Valley Parkway, Malvern, PA 19355

**Publisher's Disclaimer:** This Author Accepted Manuscript is a PDF file of an unedited peer-reviewed manuscript that has been accepted for publication but has not been copyedited or corrected. The official version of record that is published in the journal is kept up to date and so may therefore differ from this version.

### CONFLICT OF INTEREST

The authors declare that they have no relevant conflicts of interest.

## Abstract

Therapeutic targeting of initiating oncogenes is the mainstay of precision medicine. Considerable efforts have been expended toward silencing MYC, which drives many human cancers including Burkitt lymphomas (BL). Yet, the effects of MYC silencing on standard-of-care therapies are poorly understood. Here we found that inhibition of MYC transcription renders B-lymphoblastoid cells refractory to chemotherapeutic agents. This suggested that in the context of chemotherapy, stabilization of Myc protein could be more beneficial than its inactivation. We tested this hypothesis by pharmacologically inhibiting glycogen synthase kinase 3 $\beta$  (GSK-3 $\beta$ ), which normally targets Myc for proteasomal degradation. We discovered that chemorefractory BL cell lines responded better to doxorubicin and other anti-cancer drugs when Myc was thus stabilized. *In vivo*, GSK3 inhibitors (GSK3i) enhanced doxorubicin-induced apoptosis in BL patient-derived xenografts (BL-PDX) as well as in murine MYC-driven lymphoma allografts. This enhancement was accompanied by and required deregulation of several key genes acting in the extrinsic, death receptor-mediated apoptotic pathway. Consistent with this mechanism of action, GSK3i also facilitated lymphoma cell killing by a death ligand TRAIL and by a death receptor agonist mapatumumab. Thus, GSK3i synergizes with both standard chemotherapeutics and direct engagers of death receptors and could improve outcomes in patients with refractory lymphomas.

## INTRODUCTION

Therapeutic targeting of initiating oncogenes is the mainstay of precision medicine. It is thought to be most effective in cancers with a single dominant genetic event, of which Burkitt lymphoma (BL) is a prime example. BL is an aggressive subtype of non-Hodgkin's lymphoma that arises from germinal center B-cells<sup>1</sup>. The cytogenetic hallmark of BL is the t(8;14) chromosomal translocation that results in a fusion between Myc coding sequence and the immunoglobulin heavy locus (IgH) enhancer. Less commonly MYC is translocated to the immunoglobulin light chain loci, IgK or IgL<sup>2</sup>. Given the prevalence of Myc as an oncogenic driver in BL and other cancers<sup>3</sup>, numerous efforts have been made to develop Myc-targeting therapeutics<sup>4</sup>. However, in pre-clinical and clinical settings, such compounds are usually tested as monotherapies, often ignoring the question of their interactions with existing standards of care.

The interplay between Myc-targeting compounds and other anti-cancer modalities is made more complicated by the fact that Myc, while driving enhanced growth and proliferation, can also trigger cell death<sup>5,6</sup>. This occurs primarily through p53, a well-established tumor suppressor that activates intrinsic/mitochondrial apoptosis<sup>7</sup>. P53 inactivating mutations and Myc deregulation co-occur in >30% of BL tumor samples<sup>8</sup>, essentially abrogating this signaling axis and conferring chemoresistance. Not surprisingly, doxorubicin (Dox)-based EPOCH-R (etoposide, prednisone, vincristine, cyclophosphamide, and doxorubicin with rituximab) and similar regimens, which are standards of care for Burkitt and other aggressive B-lymphomas, fail to cure a significant number of patients, especially those with relapsed or refractory disease [r/r BL]<sup>9</sup>. Nevertheless, p53-independent, Myc-driven cell death has been reported by several laboratories [reviewed in<sup>5</sup>].

In principle, the pro-apoptotic activity of Myc could be leveraged for improved treatment outcomes even in chemoresistant tumors. However, apoptosis is triggered by much higher Myc levels than proliferation<sup>10</sup>. Thus, there could be proliferation without apoptosis but not apoptosis without proliferation. A potential solution to this problem is to transiently increase Myc levels immediately prior to chemotherapy, reap therapeutic benefits, and then allow Myc to return to baseline. We and others have reported that strengthening the CD19-PI3K-AKT axis is a reliable method to boost MYC protein stability in B-lymphoid cells<sup>11-13</sup>. This finding is consistent with the propensity of glycogen synthase kinase 3 beta (GSK-3 $\beta$ ), which is inhibited by Akt, to phosphorylate Myc at Thr-58, which marks Myc for recognition by the E3 ubiquitin ligase Fbxw7 and subsequent degradation [reviewed in<sup>14</sup>]. Here we report that adding GSK-3 $\beta$  inhibitors to Dox significantly improves therapeutic apoptosis in B-cell lymphomas with inactive p53 and dissect the underlying molecular mechanisms.

## **MATERIALS AND METHODS (For additional details, see Supplemental Methods)**

### **Cell culturing**

Burkitt lymphoma and B-lymphoid cell lines were cultured and maintained in RPMI 1640 medium supplemented with 10% fetal bovine serum (FBS), 2mM L-glutamine, penicillin/streptomycin (p/s) at 37°C and 5% CO<sub>2</sub>. P493-6 cells and Burkitt lymphoma cell lines Ramos, Daudi, Raji, and Mutul were acquired from Drs. Chi Dang and Riccardo Dalla-Favera. P493-6 cells were authenticated in 2010 through targeted resequencing of the transgenic *MYC* allele. P53ER/MYC cells were established and cultured as described previously<sup>15, 16</sup>. PDX MAP-GR-C95-BL-1 cells were cultured in RPMI 1640 medium supplemented with 2% FBS, 2mM L-glutamine, p/s, and 2% glucose at 37°C and 5% CO<sub>2</sub>.

### **Cytotoxicity and caspase activity assays**

For cytotoxicity assays,  $8 \times 10^4$  cells or  $5 \times 10^5$  cells (for p493-6 p53shRNA) per well of a 96-well plate were treated in triplicate with DMSO, 3  $\mu$ M CHIR, or 5 ng/mL tetracycline and indicated concentrations of Dox or TRAIL. After 48-72 hours, cell viability was measured using CellTiter-Glo (Promega, G7570) according to the manufacturer's protocol. Luminescent signal was read using a Synergy 2 plate reader (BioTek Instruments, Winooski, VT, USA). GraphPad Prism software (version 7) was used for log-transformed nonlinear regression curve fitting (4 parameter analysis). For caspase activity assays, cells were treated with DMSO or 3  $\mu$ M CHIR and indicated concentrations of Dox or vincristine.  $5 \times 10^4$  cells were plated in triplicate in a 96-well plate and caspase activity was measured using Caspase-Glo 3/7 Assay (Promega, G8091). Signals were analyzed in a Synergy 2 plate reader.

### **Allograft and Xenograft Studies**

Syngeneic tumors of P53ER/MYC cells were established in flanks of F1 hybrid B6129PF1/J 6-8 week old female mice (Jackson Laboratories stock no. 100492) as described previously<sup>16-19</sup>. Administration of drugs was started once tumors were palpable. 8 mg/kg Dox was delivered via intraperitoneal injection. CHIR99021 was dissolved in 10% DMSO, 45%

polyethylene glycol 400 (Fisher Scientific, P167-1) and 45% of .9% NaCl (Sigma S8776) and delivered via intraperitoneal injection (100 mg/kg). All animal work was conducted under a protocol approved by the Children's Hospital of Philadelphia Animal Care and Use Committee (protocol IAC 15-000902) and by the Gustave Roussy Animal Care and Use Committee (protocol APAFIS#9399-2017032714402416v3). Xenograft tumors of PDX-MAP-GR-C95-BL-1 cells were established in flanks of ATHYM-Foxn1nu/nu 5-6 week old male mice. Once tumors became palpable, mice were treated with CHIR99021 and/or Dox as described above. The model was developed in female NSG mice of 6–8 weeks at engraftment within the project Development of Pediatric PDX Models, approved by the experimental ethic committee 26 (CEEA26—Gustave Roussy) under the number 2015032614359689v7, and in accordance with European legislation, as an ancillary study of the clinical MAPPYACTS trial ([ClinicalTrials.gov](https://clinicaltrials.gov) identifier).

### Data availability

RNA-Seq data discussed in this publication have been deposited in NCBI Gene Expression Omnibus (GEO) and are accessible through GEO accession number GSE126529.

### Statistics

Statistical analysis was performed on GraphPad Prism software (version 7) by unpaired student's t-test for two group comparisons or one-way ANOVA correcting for multiple comparisons, with similar variance between groups being compared. Error bars represent s.e.m.  $\pm$  SD, and  $P < 0.05$  was considered statistically significant. For these experiments, each group is made up of at least three samples to achieve 80% power. No randomization nor blinding of investigators was performed.

## RESULTS

### MYC Sensitizes to Doxorubicin in a Myc-repressible B-lymphoid cell model

To address the role of Myc in responses to chemotherapy, we utilized the B-lymphoid cell model p493-6, which expresses a tetracycline-repressible Myc allele and endogenous Myc<sup>20</sup>. However, these cells are TP53 wild-type and do not recapitulate the genetics of BL where p53 has been reported to be mutated at a frequency of ~30%<sup>8</sup>. To make these cells a more suitable model of r/r BL, we infected cells with lentiviruses encoding two different p53-directed shRNA hairpins and selected the best knockdown for further use (Fig. S1A, arrow). In response to Dox treatment, p53shRNA-infected cells exhibited impaired induction of p53 and also displayed a higher IC50 for Dox following 72 hours of treatment (Fig. S1B, C), making them representative of r/r BL. Of note, in the absence of a chemotherapeutic agent, we observed minimal cleavage of PARP in both 'high Myc' and 'low Myc' states, indicating the ability of this B-lymphoid cell model to tolerate fluctuations in Myc levels. Furthermore, in the 'high Myc' state, therapeutic apoptosis was quite robust, as evidenced by elevated levels of cleaved PARP (Fig. 1A, left two lanes). To our surprise, in the 'low Myc' state (Fig. 1A, right two lanes), there was minimal cleavage of PARP in response to Dox.

To measure this effect quantitatively, we treated cells with vehicle or tetracycline and increasing concentrations of Dox for 72 hours and found that 'low Myc' cells (+

tetracycline) were much more resistant to Dox as measured by a 1-log increase in the IC<sub>50</sub> (Fig. 1B, S1D). To determine whether sustained Myc expression is required for Dox sensitivity or whether acute Myc activation would suffice, we started with cells in a ‘low Myc’ state and, at the time of plating/Dox treatment, washed off tetracycline from half the cells, to allow for a quick accumulation of Myc. We found that cells with acute Myc activation (“high Myc”) were much more sensitive to Dox as measured by a >1-log decrease in the IC<sub>50</sub> (Fig. 1C, S1E). These counterintuitive data indicate that high Myc, while clearly oncogenic, is essential for Dox-mediated apoptosis. This finding prompted us to investigate how Myc could be pushed beyond the apoptotic threshold in r/r BL cells under normal growth conditions or upon exposure to chemotherapy.

### **GSK-3 $\beta$ inhibition stabilizes Myc in Burkitt lymphoma cell lines**

Since Myc is regulated post-translationally by GSK-3 $\beta$  phosphorylation on the Thr58 residue, we reasoned that treating B-lymphoid cells with GSK-3 $\beta$  inhibitors such as lithium chloride<sup>21</sup> or the more specific small molecule CHIR99021<sup>22</sup> would elevate Myc to levels sufficient to trigger cell death (Fig. 2A). We first treated a panel of BL cell lines bearing wild-type or Thr58-mutant Myc with CHIR99021.  $\beta$ -catenin, a well-known GSK-3 $\beta$  target<sup>23</sup> was stabilized in all cell lines irrespective of Myc status and thus was used as a readout for GSK3 inhibition in subsequent experiments (Fig. 2B). In contrast, only wild-type Myc was transiently stabilized by CHIR99021 treatment (Fig. 2B). This stabilization was accompanied by the loss of the inhibitory Myc-Thr58 phosphorylation. We also observed Myc stabilization in the Ramos cell line (p53 mutant, Myc wild-type) upon GSK-3 $\beta$  inhibition with lithium chloride (Fig. S2A). To determine the mechanism of Myc transient stabilization, we pre-treated Ramos cells with DMSO or CHIR99021, then blocked new mRNA synthesis with actinomycin D. We found no apparent difference in mRNA stability between treatment conditions (Fig. S2B). Ramos cells pretreated with DMSO or CHIR99021 were then exposed to cycloheximide to inhibit new protein synthesis. In DMSO treated cells, Myc protein was rapidly degraded, with almost all pre-existing protein disappearing after 80 minutes (Fig. S2C, DMSO lanes). In contrast, Myc protein in CHIR99021-treated cells was very stable, with little protein loss observed after 80 minutes (Fig. S2C, CHIR lanes). Thus, increased protein stability underlies CHIR99021-mediated increases in Myc.

Since both Myc and  $\beta$ -catenin are able to promote cell cycle progression and in some cases survival, we were concerned that treatment with CHIR99021 alone could promote neoplastic growth. To address this possibility, CHIR99021-treated Ramos cells were assessed for cell cycle distribution, nuclear membrane integrity, and mitochondrial membrane depolarization using flow cytometry for propidium iodide (PI) uptake, Annexin V, and TMRE, respectively. We found no differences in cell cycle distribution or apoptosis (Fig. S2D), suggesting that while short-term treatment with CHIR99021 is unlikely to accelerate cancer progression, it will not be effective as a monotherapy either and would have to be combined with cytotoxic drugs.

### GSK-3 $\beta$ inhibition aids chemotherapy in BL by a Myc-dependent mechanism

To determine whether GSK-3 inhibition potentiates therapeutic apoptosis, we chose a two-hour CHIR99021 pre-treatment interval, which coincides with the spike in Myc levels (Fig. 2B). Ramos cells pretreated with DMSO or CHIR99021 were exposed to Dox or vincristine. We found that CHIR99021 treatment increased activation of apoptosis by both drugs as measured by enhanced PARP cleavage (Fig. S2E, F). As expected, by flow cytometric analysis we observed an increase in cleaved caspase-3 staining between Dox alone and its combination with CHIR99021 (Fig. S2G).

We also measured apoptosis activation by the Caspase-Glo 3/7 assay, which detects the release of aminoluciferin from the cleaved caspase-3/7-specific substrate. We found that CHIR99021 boosted the activation of caspases 3/7 in response to both Dox and vincristine (Fig. S2H, I). As a result, the IC<sub>50</sub> for Dox was significantly reduced across multiple experiments (Fig. 2C, S2J). In the Burkitt lymphoma cell line Daudi (p53 mutant, Myc Thr58 wild type), CHIR99021 also reduced the IC<sub>50</sub> for Dox, albeit to a lesser degree (Fig. S2K). Collectively these data demonstrate that GSK-3 $\beta$  inhibition enhances the response of Burkitt lymphoma cells to chemotherapy.

Given that GSK-3 $\beta$  has targets other than Myc, we asked to what extent this pro-apoptotic effect was due to Myc stabilization. P493-6 p53shRNA cells were treated with vehicle or low dose tetracycline to reduce Myc levels, followed by DMSO or CHIR99021 and Dox. In vehicle-treated cells, CHIR99021 lead to increased activation of apoptosis following Dox (Fig. S3A, 'Vehicle' columns). Tetracycline-treated cells expressed around ~50% less Myc, and apoptosis following Dox alone was reduced ~50%. Despite this, CHIR99021 no longer enhanced the apoptotic response to Dox (Fig. S3A, 'Tet' columns).

In parallel, we pharmacologically inhibited Myc expression in BL cells. Because Myc is regulated at the transcriptional level by BRD4<sup>24, 25</sup>, we employed the BRD4 inhibitor iBet-151 (a.k.a. GSK1210151A)<sup>26</sup> to blunt Myc transcription in the context of CHIR99021 treatment. First, we treated Ramos cells with increasing concentrations of iBet-151 and determined that 500 nM was the lowest dose at which Myc protein levels were adequately suppressed without evidence of cell death (Fig. S3B). We then cultured Ramos cells in 500 nM iBet-151 or control media for 24 hours followed by anti-GSK-3 $\beta$  adjuvant therapy. We found that when Myc expression was reduced, the cooperation between CHIR99021 and Dox was almost fully abrogated, as evidenced by the abolishment of apoptosis markers (Fig. S3C). To measure apoptosis quantitatively, we subjected cells treated with Dox, iBet-151 + Dox, CHIR + Dox, or all three drugs to flow cytometric analysis for apoptosis marker Annexin V. We found that Dox alone did not induce apoptosis very efficiently (<15% Annexin V-positive cells), and adding iBet-151 to Dox made apoptosis even less efficient (-7% net change). Combining CHIR99021 and Dox more than doubled the percentage of Annexin V positive cells as compared to Dox alone (~30%). However, treatment with all three compounds completely blocked apoptosis (Fig. S3D).

To confirm that Myc is required for anti-GSK-3 $\beta$  adjuvant therapy, we tested it on BL cell lines Raji and MutuI that are p53/MycThr58 mutant and did not exhibit a CHIR99021-mediated increase in Myc (Fig. 2B). As anticipated, addition of CHIR99021 did not affect



the IC50 for Dox in either of these cell lines (Fig. S3E, F). Collectively, these data suggest that Myc is a key GSK-3 $\beta$  target involved in CHIR99021-facilitated sensitization to chemotherapy.

### **GSK-3 $\beta$ inhibition aids chemotherapy *in vivo* in allograft and PDX models**

To test anti-GSK-3 $\beta$  adjuvant therapy *in vivo*, we first utilized a previously generated non-transgenic p53 conditionally-deficient B-lymphoma model (dubbed ‘p53ER/MYC’) <sup>16, 19</sup> wherein bone marrow cells were isolated from p53ER<sup>TAM</sup> knock-in mice <sup>27</sup> and transduced with retrovirus expressing constitutively active Myc <sup>15</sup>. We confirmed that CHIR99021 treatment transiently stabilized Myc in p53ER/MYC cells (Fig. 3A). In the context of inactive p53 (cells grown without the estrogen receptor (ER) agonist 4-OHT), there was a notable increase in cleaved PARP and cleaved caspase-3 protein following CHIR + Dox, indicating that Myc stabilization potentiates p53-independent apoptosis in this cell model *in vitro* (Fig. 3B, quantification S4A). This pro-apoptotic effect of CHIR99021 was not seen when cells were treated in the context of functional p53 (cells grown in 4-OHT; Fig. S4B). Subsequently, p53ER/MYC allografts grown in mice without 4-OHT treatment were subjected to anti-GSK-3 $\beta$  adjuvant therapy; mice received one intraperitoneal injection of vehicle, CHIR99021, vehicle + Dox, or CHIR99021 + Dox. Tumors were harvested 24 hours later and subjected to IHC staining for cleaved caspase-3. We noted a significant increase in positive cells after CHIR99021 + Dox treatment compared to Dox alone (Fig. 3C, S4C).

We also developed a patient-derived xenograft (PDX MAP-GR-C95-BL-1) model representing a p53 mutant BL. The model is derived from the pancreatic metastasis of a refractory BL with a TP53 p.Cys135Phe mutation and LOH as well as a MYC p.Pro78Ser mutation and the subclonal presence of a t(8;14) translocation involving Myc. We confirmed the PDX p53 defect by observing minimal induction of p53 protein following Dox (Fig. S4D). We then inhibited GSK-3 in cultured MAP-GR-C95-BL-1 cells with CHIR99021 or LiCl; both resulted in transient Myc stabilization similar to other Myc WT BL cell lines tested (Fig. 4A, S4E). As in Ramos cells, CHIR99021 lowered the IC50 for Dox by roughly half a log, and this decrease in IC50 was significant across multiple experiments (Fig. 4B, S4F). To test this adjuvant therapy *in vivo*, mice bearing MAP-GR-C95-BL-1 flank xenografts were treated with one intraperitoneal injection of vehicle, Dox, or CHIR99021 + Dox; tumors were harvested 24 hours later and processed for IHC measurement of cleaved caspase-3 positive cells. Upon analysis, CHIR99021 + Dox treated tumors were significantly more positive than Dox alone- or vehicle treated tumors (Fig. 4C, S4G). These findings demonstrate that GSK-3 $\beta$  inhibition with CHIR99021 can enhance *in vivo* p53-independent apoptosis in both allograft and PDX models.

### **Anti-GSK-3 $\beta$ adjuvant therapy engages and relies on extrinsic apoptosis**

To determine the underlying mechanism downstream of Myc, we profiled CHIR99021-mediated transcriptional changes by performing RNA-Seq analysis on Ramos cells treated for 0, 3, or 6 hours with CHIR99021. We first looked for overlap between CHIR99021-induced transcriptome changes and previously reported Myc signatures in two datasets pertaining to p493-6 cells- from microarray profiling (“Psathas Affy”<sup>11</sup>) and array-based

nuclear run-on (ANRO) assay (“Dang NRO”<sup>28</sup>). We compared activated genes between the three datasets and found that there were highly statistically significant overlaps between the CHIR99021 and Myc datasets, attesting to the fact that Myc is a key downstream effector of GSK-3 $\beta$  (Fig. S5A).

To examine how apoptosis-related genes were being affected, we further analyzed our RNA-seq dataset at the single gene level. We confirmed that canonical Myc targets, such as ODC1<sup>29</sup>, were being modulated as expected (Fig. S5B). We then visualized up or down-regulated KEGG apoptosis pathway genes (Fig. 5A). Of the significantly altered genes, many were related to extrinsic/death receptor-driven apoptosis, such as up-regulation of RIPK1/TNFR-*STK*, TRAIL-R4, Death Receptor 4, and down-regulation of CFLAR/FLIP, the negative regulator of extrinsic apoptosis. In contrast, intrinsic/mitochondrial apoptotic genes such as BAX, BAK, and NOXA were not significantly altered.

We validated these findings in cells treated with both CHIR99021 and Dox via qRT-PCR. Once again, we did not observe differential expression in the examined intrinsic apoptosis genes (Fig. 5B). We then re-examined expression of death receptors (Fas, TNFR1, DR4, and DR5), their cognate ligands (FasL, TNF, and TRAIL), and CFLAR/FLIP. Largely consistent with our RNA-Seq data, we observed up-regulation of DR4 and DR5, and down-regulation of CFLAR/FLIP (Fig. 5C, yellow arrows); expression of other genes was either absent (FASL; data not shown) or unaffected by CHIR99021. Interestingly, with Dox alone we saw robust upregulation of Fas and TNF, suggesting that chemotherapy alone might engage extrinsic apoptosis to some degree (Fig. 5C).

To experimentally define the role of both apoptotic pathways, we first over-expressed the pathway inhibitor Bcl-2 in Ramos cells (Fig. S5C). When we compared CHIR99021-aided apoptosis in empty vector and Bcl-2 expressing cells, we observed enhanced PARP cleavage with CHIR99021 pre-treatment in both cell lines (Fig. 6A). Furthermore, we saw significant activation of caspases-3/7 in both empty vector and Bcl-2 cells treated with CHIR99021 + Dox (Fig. S5D), although both basal and GSK3i-aided apoptosis were somewhat reduced by Bcl-2 overexpression, attesting to the involvement of the intrinsic pathway. Given that changes in intrinsic apoptosis had limited effects on therapy efficacy, we tested the contribution of the extrinsic apoptotic pathway, which is triggered by binding of death ligands to their cognate receptors and subsequent caspase activation (Fig. S5E). First, we observed that in CHIR99021 + Dox treated Ramos cells, there were higher levels of cleaved caspase-8, which is specific to extrinsic apoptosis (Fig. S5F). To test the importance of extrinsic apoptosis, we genetically manipulated members of this pathway. First, we knocked down the extrinsic adaptor protein Fadd mRNA using siRNA and subjected the cells to anti-GSK-3 $\beta$  adjuvant therapy. Despite a modest knockdown (~30%, Fig. S5G, left), therapeutic apoptosis was markedly diminished, as evidenced by reduced cleaved caspase-8 (Fig. S5G, right). To corroborate this observation, we overexpressed caspase-8 competitor CFLAR (a.k.a c-FLIP) in Ramos cells (Fig. S5H). In empty-vector cells, apoptosis could be readily induced by anti-GSK-3 $\beta$  adjuvant therapy; however, there was an almost complete abrogation of apoptosis in CFLAR/FLIP-overexpressing cells, as evidenced by a strong reduction in cleaved PARP and cleaved caspase-8 (Fig. 6B). Similarly, we saw no significant



increase in activated caspases in CFLAR/FLIP expressing cells compared to empty vector (Fig. S5I).

To analyze individual contributions of death receptors, we used the CRISPR/Cas9 system to genetically knock-out DR4 and DR5. Short guide RNAs (sgRNAs) for DR4, DR5, and a scrambled control sequence were cloned into the LentiCRISPRv2GFP lentiviral vector and stably expressed in Ramos cells. GFP-positive cells were isolated and stained for surface expression of DR4 or DR5; the knockout (KO) lines displayed almost a complete loss of DR4/5 surface expression compared to the scrambled control (Fig. S6A). Knockout was confirmed by western blot for DR4/DR5 protein (Fig. S6B). 'Scrambled sgRNA', DR4 and DR5 KO lines were treated with DMSO or CHIR and dilutions of Dox for 72 hours. We found that knockout of either DR4 or DR5 did not affect the IC50 of DMSO + Dox compared to the scrambled control; however, in DR4 or DR5 KO lines, CHIR no longer sensitized cells to Dox, as observed across multiple experiments (Fig. 7A, S6C).

Consistent with engagement of extrinsic apoptosis, we found that CHIR99021 lowered the IC50 for the DR4/DR5 ligand TRAIL by 1 log (Fig. 7B). Additionally, we utilized the human DR4 agonist antibody mapatumumab (a.k.a. HGS-ETR1)<sup>30</sup>. Similar to the results with TRAIL, CHIR99021 sensitized Ramos cells to mapatumumab as seen by a half-log reduction in IC50 (Fig. 7C). To determine if DR4 involvement is clinically relevant, we analyzed 10 Burkitt lymphoma clinical samples for IHC expression of DR4 and compared them to 5 normal tonsils. We found that while in the tonsillar germinal center the staining was very weakly cytoplasmic, the lymphoma samples displayed robust membrane and cytoplasmic staining (Fig. S6D). Collectively these data demonstrate that GSK-3 $\beta$  inhibition potentiates the apoptotic activity of death receptors such as DR4 and reveals the critical dependence of anti-GSK-3 $\beta$  adjuvant therapy on extrinsic apoptosis.

## DISCUSSION

Our studies using murine allografts and human Burkitt lymphoma cell lines and PDXs demonstrate the benefits of adding GSK3 inhibitors to chemotherapeutic drugs in the R-CHOP/EPOCH-R regimens. They also firmly implicate Myc as the key downstream target of GSK-3 $\beta$  and a master regulator of chemosensitivity in refractory B-cell lymphomas. Finally, we have learned that Myc-dependent chemosensitivity relies on the extrinsic apoptotic pathway, with direct involvement of death receptors such as DR4, whose ligands and agonists function better when GSK-3 $\beta$  is inhibited and Myc is stabilized (Fig. 8). All three key conclusions would be impossible to predict in theory because both GSK-3 $\beta$  and Myc have multitudes of targets with non-overlapping and often conflicting functions.

### GSK-3 $\beta$ and therapeutic apoptosis

The literature on the role of GSK-3 $\beta$  in modulating apoptosis is complex, with some evidence that GSK-3 $\beta$  inhibits the extrinsic apoptotic pathway through an unidentified mechanism, while potentiating the intrinsic pathway [reviewed in<sup>31</sup>]. Thus, its overall contribution to cell survival in the face of genotoxic therapy remains controversial and likely cell type-specific. A 2008 study demonstrated that GSK-3 $\beta$  inhibition in glioblastoma multiforme results in decreased NF- $\kappa$ B activity<sup>32</sup>. Simultaneously, another group reported

the beneficial effects of targeting GSK-3 $\beta$  in a preclinical murine model of MLL leukemia, with the underlying mechanism being stabilization of the cyclin-dependent kinase inhibitor p27<sup>33</sup>. Another firmly established GSK-3 $\beta$  target is PTEN, which is phosphorylated by this kinase on Thr-366 and Ser-362<sup>34</sup>. While Thr366 phosphorylation is thought to lead to PTEN destabilization<sup>35</sup>, the contribution of Ser-362 phosphorylation to PTEN function is not known. Given that this tumor suppressor is known to contribute to both intrinsic survival pathways<sup>36</sup> and the extrinsic cell death pathways<sup>37, 38</sup>, the overall effect of GSK3i on therapeutic apoptosis in B-lymphoid malignancies would have been difficult to predict with certainty. The fact that one of its key targets Myc has manifold effects on tumor cell survival only adds to the complexity of this system.

### **Myc and extrinsic apoptosis**

The role of Myc in cell death has been incompletely understood, despite the large amount of published studies. While Myc is best known to induce p53-dependent, intrinsic apoptosis, Myc has also been linked to the extrinsic pathway. Notably, it has been shown to participate in apoptosis induced by CD95/CD95L (Fas/FasL)<sup>39</sup> as well as TNF $\alpha$ <sup>40</sup>. Our earlier work reported the relationship between inhibition of GSK-3 $\beta$  and subsequent increase in Myc and enhanced apoptosis in vitro in response to TRAIL<sup>41</sup>, at least in part through the propensity of Myc to directly inhibit CFLAR/c-FLIP<sup>42, 43</sup>. In parallel, in some solid cancers Myc elevates expression of the death receptors DR4 and DR5 and the extrinsic ligand FasL<sup>44-46</sup>.

While these data, in particular regarding CFLAR/c-FLIP, are consistent with the pro-apoptotic function of Myc, there are reports challenging the notion that there is a linear correlation between FLIP levels and TRAIL resistance [see for example<sup>47</sup>]. In addition, our RNA-Seq experiment demonstrated that in Myc-stabilized cells other transcripts went in the opposite, pro-survival direction, with strong downregulation of TNFR1, Fas, and TRAIL. Thus, one could have predicted that stabilization of Myc would limit cell death and by inference confer chemoresistance – or that the effects of Myc on the extrinsic pathway would be irrelevant in the context of genotoxic chemotherapy.

### **Apoptosis-related mechanisms of chemoresistance**

Traditionally, chemoresistance is seen as a failure of the intrinsic pathway. This view is based on the fact that many pro- and anti-apoptotic members of the intrinsic pathway are altered in cancer. For example, IAPs (inhibitors of apoptosis proteins) frequently confer survival to neoplastic cells, especially when overexpressed in tumor cells<sup>48</sup>. Furthermore, the expression and mutation status of Bcl-2 family members is predictive of responses to chemotherapy prognosis: both mutations in the pro-apoptotic gene BAX and over-expression of BCL-2 are common in many cancer types<sup>49</sup>. Therefore, the small molecular inhibitor of Bcl-2 venetoclax has shown considerable promise in preclinical and clinical trials, including those involving B-lymphoid malignancies<sup>50</sup>.

Despite an established role for intrinsic apoptosis in resistance to chemotherapy, there is also a body of evidence that points to the importance of extrinsic apoptosis for responses to chemotherapy. Published data show that signaling through the death receptor CD95/Fas is critical for chemosensitivity<sup>51</sup>. Conversely, resistance to chemotherapy in leukemia and

other cancers can be attributed to downregulation of this death receptor<sup>52</sup>. In addition, mutations in CD95 have been identified in many solid and hematopoietic tumors [reviewed in<sup>53</sup>]. Finally, upregulation of CFLAR/c-FLIP and its increased recruitment to CD95 has been observed in response to various chemotherapeutics in B-ALL and in fact is a resistance mechanism to chemotherapy treatment<sup>54</sup>.

Utilizing Ramos Burkitt lymphoma cells, we observed robust upregulation of Fas mRNA in response to treatment with Dox, while there were minimal changes in intrinsic apoptosis genes. Over-expression of Bcl-2 conferred a very modest decrease in Dox induced apoptosis (~30% inhibition of caspase 3/7 activity). In contrast, we observed a sharp increase in chemoresistance via overexpression of CFLAR/c-FLIP or by CRISPR/Cas9 knockout of extrinsic death receptors DR4 or DR5.

### Implications for anti-cancer therapeutics

Data presented throughout the paper suggest that even in the absence of p53, stabilized Myc belongs firmly on the “cell death” side. Notably, when we inhibited Myc transcription with the Brd4 inhibitor iBet-151 at a sub-lethal concentration, there was actually a reduction in GSK3i-aided apoptosis. Thus, in the context of chemotherapy regimens, inactivation of Myc would be counterproductive, as Myc potentiates doxorubicin-induced cell death by engaging extrinsic apoptosis. This observation adds a new wrinkle to the prevailing view that Myc contributes to B-lymphoma cell survival in the face of chemotherapy [see for example<sup>55</sup>].

The results of our studies also suggest several new ways to improve upon standard-of-care therapies for Myc-driven B-cell lymphomas. First, our data suggest that the addition of a GSK-3 $\beta$  inhibitor (LiCl, CHIR99021, or tideglusib currently in Phase II clinical trials for Alzheimer’s disease) could enhance the response to chemotherapy even in cells where the intrinsic apoptotic pathway is suppressed. Two such subtypes of B-cell lymphoma associated with poor response to therapy are double- and triple hit lymphomas (Myc and Bcl-2/Bcl-6 translocated)<sup>56</sup> as well as non-translocated lymphomas double-positive for Myc and Bcl-2<sup>57</sup>. Second, our findings that anti-GSK-3 $\beta$  adjuvant therapy engages extrinsic apoptosis provides a rationale for revisiting clinical trials of soluble TRAIL or agonistic antibodies targeting DR4 and DR5. Trials with recombinant TRAIL demonstrated safety and tolerability but there was no observed anti-cancer activity in combination with standard-of-care for the cancer types treated. Similarly, with trials using agonistic TRAIL receptor antibodies in combination with standards-of-care, there was a trend towards anti-cancer activity but no statistically significant results<sup>58</sup>. However, GSK-3 $\beta$  inhibition and ensuing Myc stabilization could make tumor cells more susceptible to the pro-apoptotic actions of TRAIL or death receptor targeting antibodies such as mapatumumab<sup>59</sup>. Finally, the potential to re-purpose the FDA approved GSK-3 $\beta$  inhibitor lithium chloride makes this adjuvant therapy strategy particularly viable as the process to transition this psychiatric drug to cancer therapy would be relatively unchallenging. Long-term usage of lithium chloride is not correlated with an increase in cancer incidence so it appears to be a safe adjuvant<sup>60</sup>.

### Supplementary Material

Refer to Web version on PubMed Central for supplementary material.

## ACKNOWLEDGEMENTS

The authors thank the members of their laboratories and CHOP Research Institute Normal and Malignant Hematopoiesis Research Affinity Group for stimulating discussions, and Daniel Martinez and the CHOP Pathology Core for assistance in IHC stain analysis. iBet-151 was a kind gift from Dr. Olena Barbash (GlaxoSmithKline) and was first tested in our lab by Daniel Soto de Jesus (University of Pennsylvania). This work was supported by the V Foundation for Cancer Research, the NIH grants R01CA196299 & R21 CA183445 (ATT), R01 HL110806 (PK), T32 GM007229 & F31 CA217004 (CTH), and the Institut National du Cancer grant PL-BIO 2016-179 (JW). The MAPPYACTS protocol is supported by the Institut National du Cancer grant PHRC-K14-175 and the Fondation ARC grant MAPY201501241. The PDX development is supported and aided by the Société Française de Lutte contre les Cancers et les Leucémies de l'Enfant et l'Adolescent (Fondation Enfants et Santé), the Fondation AREMIG, the Association Thibault BRIET, and the Gustave Roussy animal care facility (Karine Ser-Leroux).

## REFERENCES

1. Dave SS, Fu K, Wright GW, Lam LT, Kluin P, Boerma EJ, et al. Molecular diagnosis of Burkitt's lymphoma. *N Engl J Med* 2006 6/8/2006; 354(23): 2431–2442. [PubMed: 16760443]
2. Dalla-Favera R, Martinotti S, Gallo RC, Erikson J, Croce CM. Translocation and rearrangements of the c - myc oncogene locus in human undifferentiated B-cell lymphomas. *Science* 1983 2/25/1983; 219(4587): 963–967. [PubMed: 6401867]
3. Dang CV. MYC, Metabolism, Cell Growth, and Tumorigenesis. *Cold Spring Harbor Perspectives in Medicine* 2013 8 1, 2013; 3(8).
4. McKeown MR, Bradner JE. Therapeutic strategies to inhibit MYC. *Cold Spring Harb Perspect Med* 2014 10 1; 4(10).
5. McMahon SB. MYC and the control of apoptosis. *Cold Spring Harb Perspect Med* 2014 7 1, 2014; 4(7).
6. Hann SR. MYC Cofactors: Molecular Switches Controlling Diverse Biological Outcomes. *Cold Spring Harbor Perspectives in Medicine* 2014 9 1, 2014; 4(9).
7. Zindy F, Eischen CM, Randle DH, Kamijo T, Cleveland JL, Sherr CJ, et al. Myc signaling via the ARF tumor suppressor regulates p53-dependent apoptosis and immortalization. *Genes Dev* 1998 8/1/1998; 12(15): 2424–2433. [PubMed: 9694806]
8. Cheung KJ, Horsman DE, Gascoyne RD. The significance of TP53 in lymphoid malignancies: mutation prevalence, regulation, prognostic impact and potential as a therapeutic target. *Br J Haematol* 2009 8; 146(3): 257–269. [PubMed: 19500100]
9. Dunleavy K, Noy A, Abramson JS, LaCasce AS, Link BK, Parekh S, et al. Risk-Adapted Therapy in Adults with Burkitt Lymphoma: Preliminary Report of a Multicenter Prospective Phase II Study of DA -EPOCH-R. *Blood* 2015; 126(23): 342–342.
10. Murphy DJ, Junttila MR, Pouyet L, Karnezis A, Shchors K, Bui DA, et al. Distinct thresholds govern Myc's biological output in vivo. *Cancer Cell* 2008 12/9/2008; 14(6): 447–457. [PubMed: 19061836]
11. Psathas JN, Doonan PJ, Raman P, Freedman BD, Minn AJ, Thomas-Tikhonenko A. The Myc-miR-17-92 axis amplifies B-cell receptor signaling via inhibition of ITIM proteins: a novel lymphomagenic feed-forward loop. *Blood* 2013 12 19; 122(26): 4220–4229. [PubMed: 24169826]
12. Chung EY, Psathas JN, Yu D, Li Y, Weiss MJ, Thomas-Tikhonenko A. CD19 is a major B cell receptor-independent activator of MYC-driven B-lymphomagenesis. *J Clin Invest* 2012 5 1; 122(6): 2257–2266. [PubMed: 22546857]
13. Sander S, Calado Dinis P, Srinivasan L, Köchert K, Zhang B, Rosolowski M, et al. Synergy between PI3K Signaling and MYC in Burkitt Lymphomagenesis. *Cancer Cell* 2012; 22(2): 167–179. [PubMed: 22897848]
14. Farrell AS, Sears RC. MYC Degradation. *Cold Spring Harbor Perspectives in Medicine* 2014 3 1, 2014; 4(3).
15. Yu D, Thomas-Tikhonenko A. A non-transgenic mouse model for B-cell lymphoma: in vivo infection of p53-null bone marrow progenitors by a Myc retrovirus is sufficient for tumorigenesis. *Oncogene* 2002 2002; 21(12): 1922–1927. [PubMed: 11896625]

16. Amaravadi RK, Yu D, Lum JJ, Bui T, Christophorou MA, Evan GI, et al. Autophagy inhibition enhances therapy-induced apoptosis in a Myc-induced model of lymphoma. *J Clin Invest* 2007 1/18/2007; 117 (2): 326–336. [PubMed: 17235397]
17. Yu D, Cozma D, Park A, Thomas-Tikhonenko A. Functional validation of genes implicated in lymphomagenesis: an in vivo selection assay using a Myc-induced B-cell tumor. *Annals NY Acad Sci* 2005 2005; 1059: 145–159.
18. Yu D, Dews M, Park A, Tobias JW, Thomas-Tikhonenko A. Inactivation of Myc in two-hit B-lymphomas causes dormancy with elevated levels of interleukin-10 receptor and CD20: implications for adjuvant therapies. *Cancer Res* 2005 2005; 65(12): 5454–5461. [PubMed: 15958595]
19. Yu D, Carroll M, Thomas-Tikhonenko A. p53 status dictates responses of B-lymphomas to monotherapy with proteasome inhibitors. *Blood* 2007 2/6/2007; 109(11): 4936–4943. [PubMed: 17284530]
20. Pajic A, Spitkovsky D, Christoph B, Kempkes B, Schuhmacher M, Staeger MS, et al. Cell cycle activation by c-myc in a Burkitt lymphoma model cell line. *Int J Cancer* 2000 9 15; 87 (6): 787–793. [PubMed: 10956386]
21. O'Brien WT, Klein PS. Validating GSK3 as an in vivo target of lithium action. *Biochem Soc Trans* 2009 10/2009; 37(Pt 5): 1133–1138.
22. Ring DB, Johnson KW, Henriksen EJ, Nuss JM, Goff D, Kinnick TR, et al. Selective glycogen synthase kinase 3 inhibitors potentiate insulin activation of glucose transport and utilization in vitro and in vivo. *Diabetes* 2003 3; 52(3): 588–595. [PubMed: 12606497]
23. Aberle H, Bauer A, Stappert J, Kispert A, Kemler R. beta-catenin is a target for the ubiquitin-proteasome pathway. *EMBO J* 1997 7/1/1997; 16(13): 3797–3804. [PubMed: 9233789]
24. Delmore JE, Issa GC, Lemieux ME, Rahl PB, Shi J, Jacobs HM, et al. BET bromodomain inhibition as a therapeutic strategy to target c-Myc. *Cell* 2011 9/16/2011; 146(6): 904–917. [PubMed: 21889194]
25. Zuber J, Shi J, Wang E, Rappaport AR, Herrmann H, Sison EA, et al. RNAi screen identifies Brd4 as a therapeutic target in acute myeloid leukaemia. *Nature* 2011 10/27/2011; 478(7370): 524–528. [PubMed: 21814200]
26. Dawson MA, Prinjha RK, Dittmann A, Giotopoulos G, Bantscheff M, Chan WI, et al. Inhibition of BET recruitment to chromatin as an effective treatment for MLL-fusion leukaemia. *Nature* 2011 10/27/2011; 478(7370): 529–533. [PubMed: 21964340]
27. Christophorou MA, Martin-Zanca D, Soucek L, Lawlor ER, Brown-Swigart L, Verschuren EW, et al. Temporal dissection of p53 function in vitro and in vivo. *Nat Genet* 2005 7/2005; 37(7): 718–726. [PubMed: 15924142]
28. Fan J, Zeller K, Chen YC, Watkins T, Barnes KC, Becker KG, et al. Time-dependent c-Myc transactomes mapped by Array-based nuclear run-on reveal transcriptional modules in human B cells. *PLoS One* 2010 3 15; 5(3): e9691. [PubMed: 20300622]
29. Bello-Fernandez C, Packham G, Cleveland JL. The ornithine decarboxylase gene is a transcriptional target of c-Myc. *Proc Natl Acad Sci USA* 1993 1993; 90: 7804–7808. [PubMed: 8356088]
30. Pukac L, Kanakaraj P, Humphreys R, Alderson R, Bloom M, Sung C, et al. HGS-ETR1, a fully human TRAIL-receptor 1 monoclonal antibody, induces cell death in multiple tumour types in vitro and in vivo. *Brit J Cancer* 2005 4/20/online; 92: 1430–1441. [PubMed: 15846298]
31. Beurel E, Jope RS. The paradoxical pro- and anti-apoptotic actions of GSK3 in the intrinsic and extrinsic apoptosis signaling pathways. *Prog Neurobiol* 2006 7; 79(4): 173–189. [PubMed: 16935409]
32. Kotliarova S, Pastorino S, Kovell LC, Kotliarov Y, Song H, Zhang W, et al. Glycogen synthase kinase-3 inhibition induces glioma cell death through c-MYC, nuclear factor-kappaB, and glucose regulation. *Cancer Res* 2008 8 15; 68(16): 6643–6651. [PubMed: 18701488]
33. Wang Z, Smith KS, Murphy M, Piloto O, Somerville TC, Cleary ML. Glycogen synthase kinase 3 in MLL leukaemia maintenance and targeted therapy. *Nature* 2008 10 30; 455(7217): 1205–1209. [PubMed: 18806775]

34. Al-Khouri AM, Ma Y, Togo SH, Williams S, Mustelin T. Cooperative phosphorylation of the tumor suppressor phosphatase and tensin homologue (PTEN) by casein kinases and glycogen synthase kinase 3beta. *J Biol Chem* 2005 10 21; 280(42): 35195–35202. [PubMed: 16107342]
35. Maccario H, Perera NM, Davidson L, Downes CP, Leslie NR. PTEN is destabilized by phosphorylation on Thr366. *Biochem J* 2007 8 1; 405(3): 439–444. [PubMed: 17444818]
36. Stambolic V, Suzuki A, de la Pompa JL, Brothers GM, Mirtsos C, Sasaki T, et al. Negative regulation of PKB/Akt-dependent cell survival by the tumor suppressor PTEN. *Cell* 1998 10 2; 95(1): 29–39. [PubMed: 9778245]
37. Jayarama S, Li LC, Ganesh L, Mardi D, Kanteti P, Hay N, et al. MADD is a downstream target of PTEN in triggering apoptosis. *J Cell Biochem* 2014 2; 115(2): 261–270. [PubMed: 24038283]
38. Yuan XJ, Whang YE. PTEN sensitizes prostate cancer cells to death receptor-mediated and drug-induced apoptosis through a FADD-dependent pathway. *Oncogene* 2002 1 10; 21(2): 319–327. [PubMed: 11803475]
39. Hueber AO, Zornig M, Lyon D, Suda T, Nagata S, Evan GI. Requirement for the CD95 receptor-ligand pathway in c-Myc-induced apoptosis. *Science* 1997 11/14/1997; 278(5341): 1305–1309. [PubMed: 9360929]
40. Klefstrom J, Vastrik I, Saksela E, Valle J, Eilers M, Alitalo K. c-Myc induces cellular susceptibility to the cytotoxic action of TNF-alpha. *EMBO J* 1994 11/15/1994; 13(22): 5442–5450. [PubMed: 7957110]
41. Mayes PA, Dolloff NG, Daniel CJ, Liu JJ, Hart LS, Kuribayashi K, et al. Overcoming hypoxia-induced apoptotic resistance through combinatorial inhibition of GSK-3beta and CDK1. *Cancer Res* 2011 8/1/2011; 71(15): 5265–5275. [PubMed: 21646472]
42. Ricci MS, Kim SH, Ogi K, Plastaras JP, Ling J, Wang W, et al. Reduction of TRAIL-induced Mcl-1 and cIAP2 by c-Myc or sorafenib sensitizes resistant human cancer cells to TRAIL-induced death. *Cancer Cell* 2007 7; 12(1): 66–80. [PubMed: 17613437]
43. Ricci S, Jin Z, Dews M, Yu D, Thomas-Tikhonenko A, Dicker DT, et al. Direct repression of FLIP expression by c-myc is a major determinant of TRAIL sensitivity. *Mol Cell Biol* 2004; 24(19): 8541–8555. [PubMed: 15367674]
44. Sussman RT, Ricci MS, Hart LS, Sun SY, El-Deiry WS. Chemotherapy-resistant side-population of colon cancer cells has a higher sensitivity to TRAIL than the non-SP, a higher expression of c-Myc and TRAIL-receptor DR4. *Cancer Biol Ther* 2007 9; 6(9): 1490–1495. [PubMed: 17881904]
45. Wang Y, Engels IH, Knee DA, Nasoff M, Deveraux QL, Quon KC. Synthetic lethal targeting of MYC by activation of the DR5 death receptor pathway. *Cancer Cell* 2004 5; 5(5): 501–512. [PubMed: 15144957]
46. Kasibhatla S, Beere HM, Brunner T, Echeverri F, Green DR. A 'non-canonical' DNA-binding element mediates the response of the Fas-ligand promoter to c-Myc. *Curr Biol* 2000 10 5; 10(19): 1205–1208. [PubMed: 11050389]
47. Chang DW, Xing Z, Pan Y, Algeciras-Schimmich A, Barnhart BC, Yaish-Ohad S, et al. c-FLIP(L) is a dual function regulator for caspase-8 activation and CD95-mediated apoptosis. *EMBO J* 2002 7/15/2002; 21(14): 3704–3714. [PubMed: 12110583]
48. Fulda S, Vucic D. Targeting IAP proteins for therapeutic intervention in cancer. *Nat Rev Drug Discov* 2012 2 01; 11(2): 109–124. [PubMed: 22293567]
49. Yip KW, Reed JC. Bcl-2 family proteins and cancer. *Oncogene* 2008 10 27; 27(50): 6398–6406. [PubMed: 18955968]
50. Roberts AW, Davids MS, Pagel JM, Kahl BS, Puvvada SD, Gerecitano JF, et al. Targeting BCL2 with Venetoclax in Relapsed Chronic Lymphocytic Leukemia. *N Engl J Med* 2016 1 28; 374(4): 311–322. [PubMed: 26639348]
51. Müller M, Wilder S, Bannasch D, Israeli D, Lehlbach K, Li-Weber M, et al. p53 activates the CD95 (APO-1/Fas) gene in response to DNA damage by anticancer drugs. *J Exp Med* 1998 12 7; 188(11): 2033–2045. [PubMed: 9841917]
52. Friesen C, Fulda S, Debatin KM. Deficient activation of the CD95 (APO-1/Fas) system in drug-resistant cells. *Leukemia* 1997 11; 11(11): 1833–1841. [PubMed: 9369415]
53. Debatin KM, Stahnke K, Fulda S. Apoptosis in hematological disorders. *Semin Cancer Biol* 2003 4; 13(2): 149–158. [PubMed: 12654258]



54. Troeger A, Schmitz I, Siepermann M, Glouchkova L, Gerdemann U, Janka-Schaub GE, et al. Up-regulation of c-FLIP<sub>S+R</sub> upon CD40 stimulation is associated with inhibition of CD95-induced apoptosis in primary precursor B-ALL. *Blood* 2007 7 1; 110(1): 384–387. [PubMed: 17376892]
55. Culjkovic-Kraljacic B, Fernando TM, Marullo R, Calvo-Vidal N, Verma A, Yang S, et al. Combinatorial targeting of nuclear export and translation of RNA inhibits aggressive B-cell lymphomas. *Blood* 2016 2 18; 127 (7): 858–868. [PubMed: 26603836]
56. Johnson NA, Savage KJ, Ludkovski O, Ben-Neriah S, Woods R, Steidl C, et al. Lymphomas with concurrent BCL2 and MYC translocations: the critical factors associated with survival. *Blood* 2009 9 10; 114(11): 2273–2279. [PubMed: 19597184]
57. Hu S, Xu-Monette ZY, Tzankov A, Green T, Wu L, Balasubramanyam A, et al. MYC/BCL2 protein coexpression contributes to the inferior survival of activated B-cell subtype of diffuse large B-cell lymphoma and demonstrates high-risk gene expression signatures: a report from The International DLBCL Rituximab-CHOP Consortium Program. *Blood* 2013 5 16; 121(20): 4021–4031. [PubMed: 23449635]
58. Lemke J, von Karstedt S, Zinngrebe J, Walczak H. Getting TRAIL back on track for cancer therapy. *Cell Death Differ* 2014 9; 21(9): 1350–1364. [PubMed: 24948009]
59. Maddipatla S, Hernandez-Ilizaliturri FJ, Knight J, Czuczman MS. Augmented antitumor activity against B-cell lymphoma by a combination of monoclonal antibodies targeting TRAIL-R1 and CD20. *Clin Cancer Res* 2007 8 1; 13(15 Pt 1): 4556–4564. [PubMed: 17671142]
60. Cohen Y, Chetrit A, Cohen Y, Sirota P, Modan B. Cancer morbidity in psychiatric patients: influence of lithium carbonate treatment. *Med Oncol* 1998 4; 15(1): 32–36. [PubMed: 9643528]

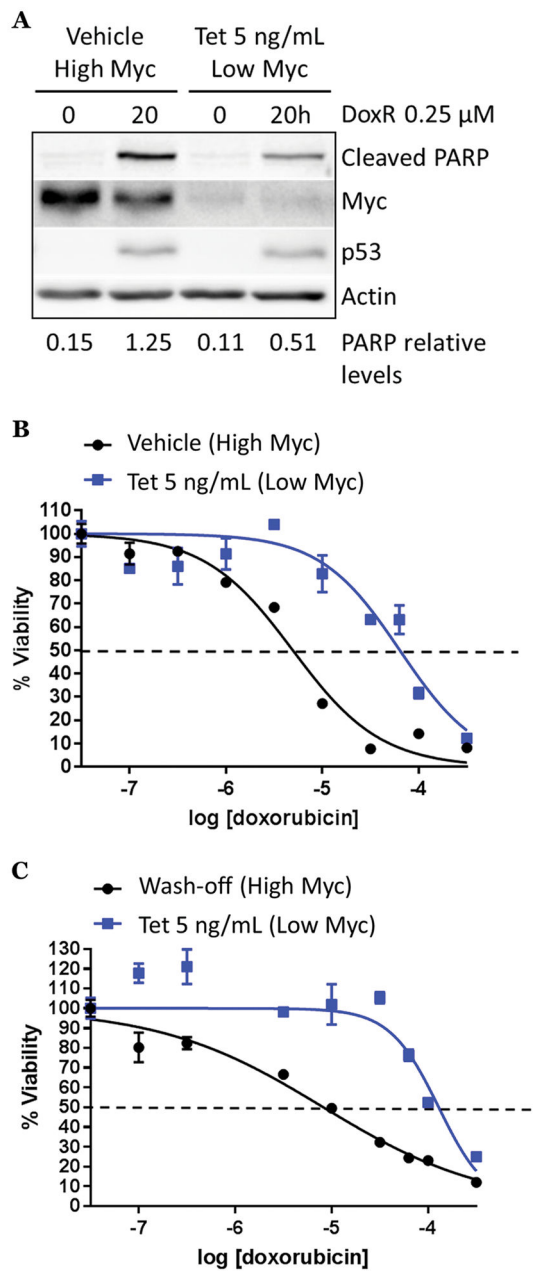


**Figure 1. Myc is critical for doxorubicin sensitivity in a Myc-repressible B-lymphoid model.** **A)** p493-6 p53shRNA cells were treated with vehicle (high Myc) or 5 ng/mL tetracycline (low Myc) for 5 hours and doxorubicin as indicated. Western blotting was performed for cleaved PARP, Myc, p53 and acting loading control. Levels of cleaved PARP (indicated below) were quantified using Image J software and plotted with GraphPad Prism. **B)** 72 hour Dox dose response curve of p493-6 p53shRNA cells treated with 5 ng/mL tetracycline or vehicle; survival was assessed using CellTiter-Glo and plotted on GraphPad Prism. **C)** P493-6 p53shRNA cells were treated with 5 ng/mL tetracycline or vehicle overnight. The next day, tet was removed from half of the cells. All cells were then treated with increasing concentrations of doxorubicin for 48 hours and cell survival was measured as in B).

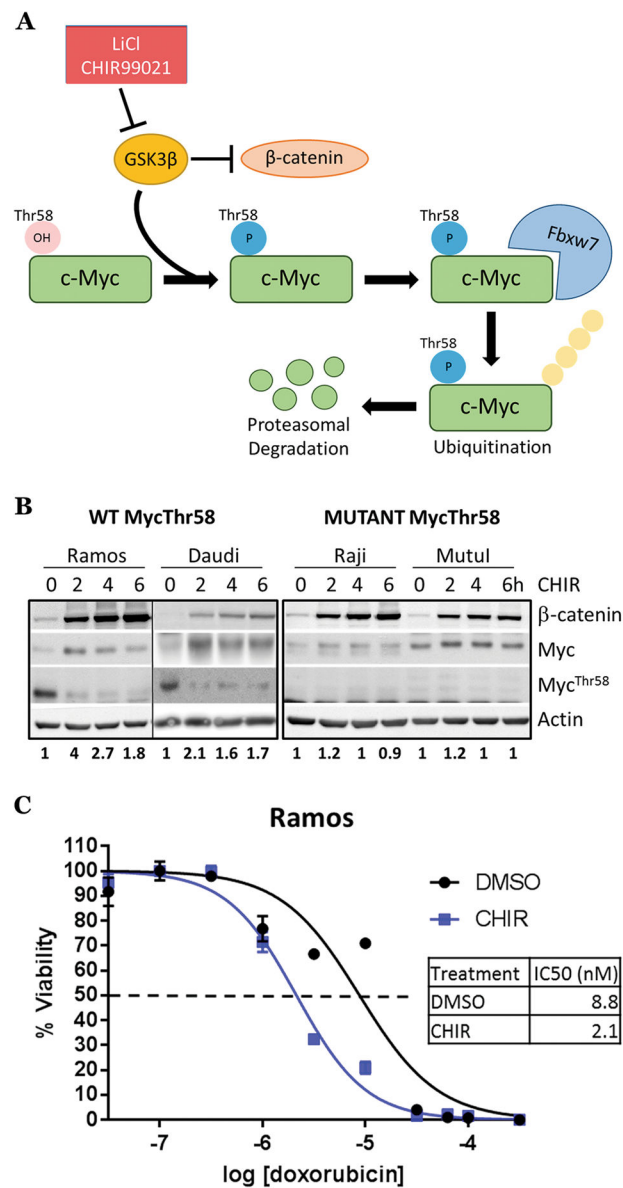


**Figure 2. GSK-3 $\beta$  inhibition stabilizes Myc and increases sensitivity to chemotherapy in Myc wild-type Burkitt lymphoma cell lines.**

**A)** Model of Myc protein regulation by GSK-3 $\beta$ . **B)** Myc wild type (left) & Thr58 mutant (right) Burkitt lymphoma cell lines were treated with 3  $\mu$ M CHIR99021 for a 6 hour time course. Western blotting was performed for  $\beta$ -catenin, Myc, Myc<sup>Thr58</sup> phosphorylation and actin control, with Myc quantification using ImageJ below. **C)** Ramos cells were treated with DMSO or 3  $\mu$ M CHIR99021 and increasing concentrations of doxorubicin for 72 hours. Cell survival was assessed as in Fig. 1B).

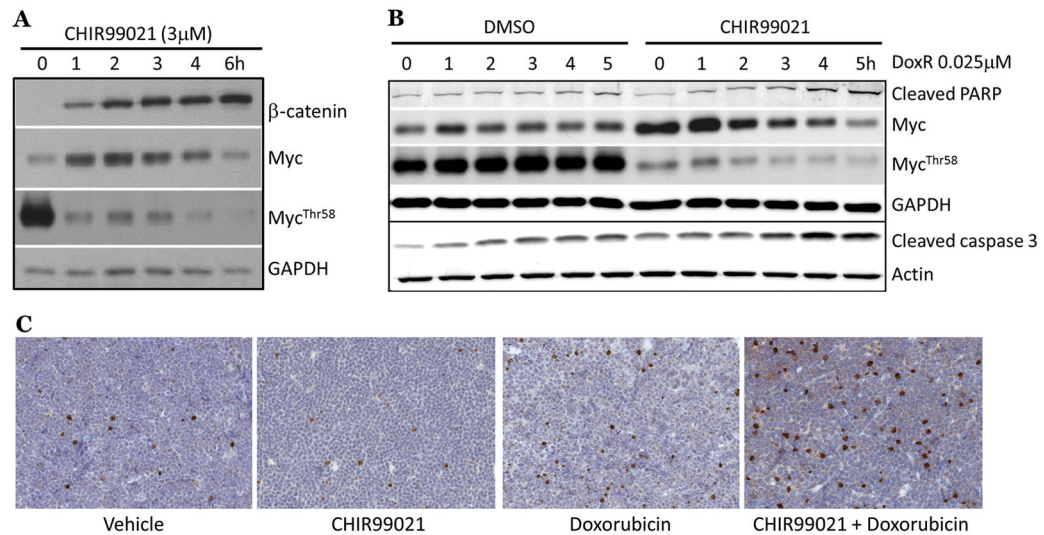


**Figure 3. GSK-3 inhibition enhances p53-independent apoptosis in syngeneic murine B-cell neoplasms.**

**A)** p53ER/MYC cells were treated with CHIR99021 as indicated. Western blotting was performed for markers of GSK-3 $\beta$  inhibition. **B)** p53ER/MYC cells were grown without 4-OHT (p53-inactive). Cells were treated with DMSO or 3  $\mu$ M CHIR99021 for 2 hours followed by doxorubicin as indicated. Western blotting was performed for markers of GSK-3 $\beta$  inhibition, apoptosis, and loading controls. **C)** F1 hybrid B6129PF1/J mice bearing p53ER/MYC subcutaneous grafts were intraperitoneally injected with vehicle, vehicle + 8 mg/kg doxorubicin, 100 mg/kg CHIR99021, or 100 mg/kg CHIR99021 + 8 mg/kg doxorubicin. Tumors were harvested after 18 hours for immunohistochemistry (IHC). Representative images of cleaved caspase-3 stains (brown) are shown for each treatment group.

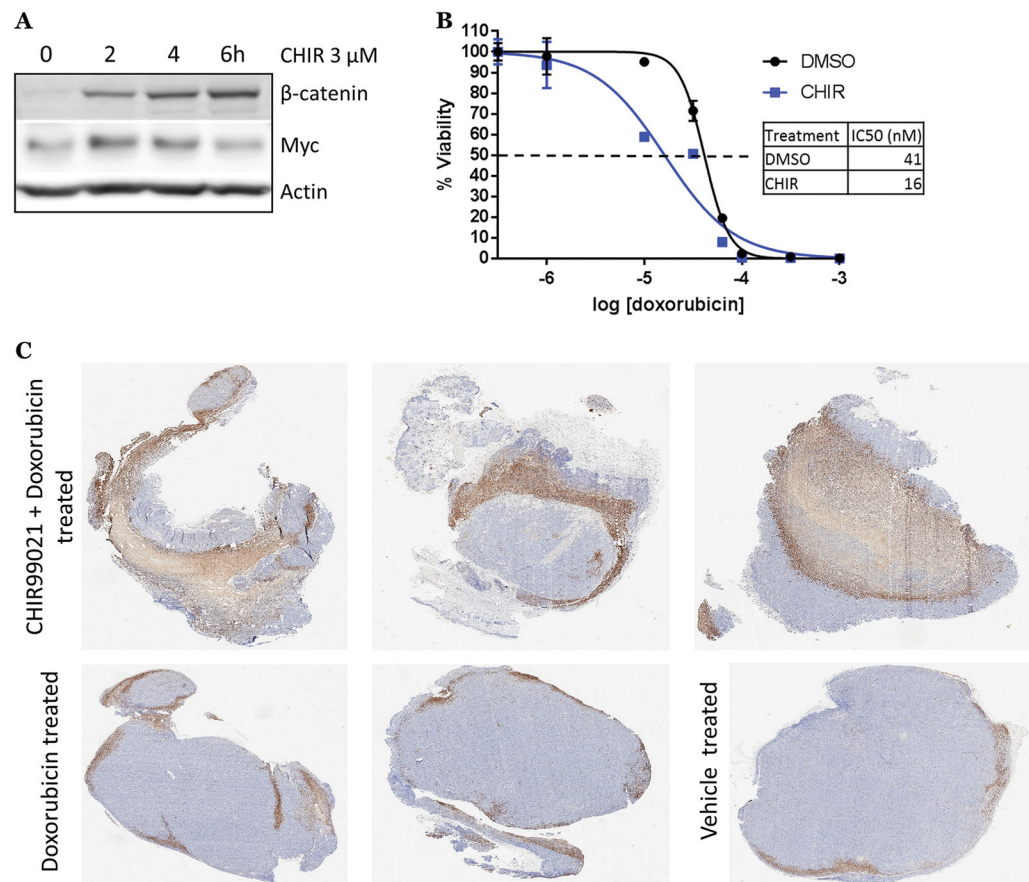


**Figure 4. GSK-3 $\beta$  inhibition increases sensitivity to chemotherapy in Burkitt lymphoma PDX.** **A)** PDX MAP-GR-C95-BL-1 cells were treated with CHIR99021 as indicated. Western blotting was performed for  $\beta$ -catenin and Myc. **B)** PDX MAP-GR-C95-BL-1 cells were treated with DMSO or 3  $\mu$ M CHIR99021 and increasing concentrations of doxorubicin for 72 hours. Cell survival was assessed as in Fig. 1B. **C)** ATHYM-Foxn1 $nu/nu$  mice bearing MAP-GR-C95-BL-1 xenografts were intraperitoneally injected with 8 mg/kg doxorubicin or 100 mg/kg CHIR99021 + 8 mg/kg doxorubicin. Tumors were harvested after 24 hours for immunohistochemistry (IHC). Representative images of whole tumors stained for cleaved caspase-3.

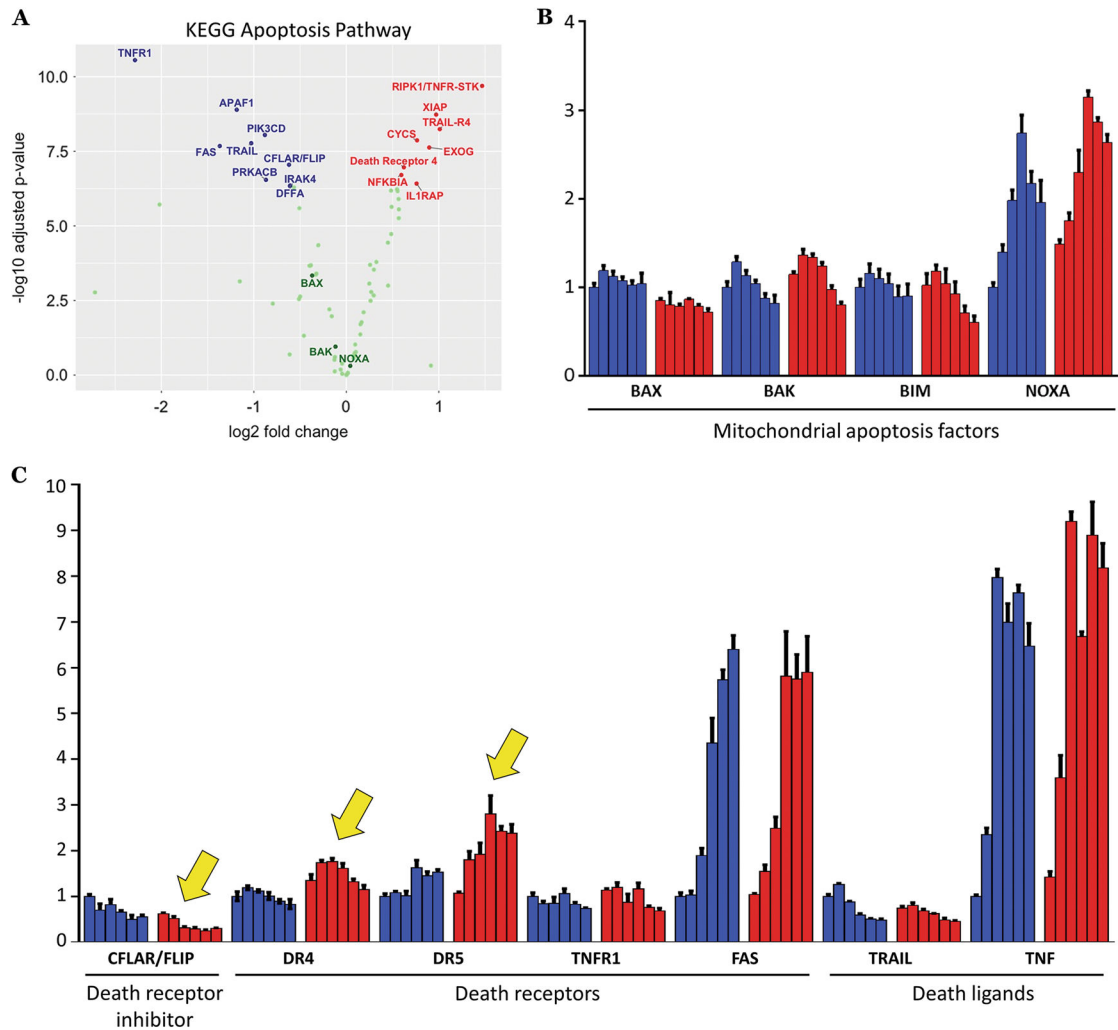


**Figure 5. GSK-3 $\beta$  inhibition alters extrinsic apoptosis genes.**

**A)** Volcano plot of KEGG apoptosis genes derived from RNA-Seq data on Ramos cells treated for 3 hours with 3  $\mu$ M CHIR99021 in biological triplicates. Key apoptotic genes are labeled, with genes in blue being down-regulated, genes in red being up-regulated, and genes in green having no significant changes. **B)** qRT-PCR expression analysis for known Myc-dependent intrinsic/mitochondrial apoptotic factors was performed on Ramos cells treated for 2 hours with DMSO (blue bars) or 3  $\mu$ M CHIR99021 (red bars) followed by a 6 hour time course of .25  $\mu$ M doxorubicin. **C)** qRT-PCR expression analysis for extrinsic apoptosis factors was performed on Ramos cells treated as in B). Notable changes are indicated with yellow arrows.



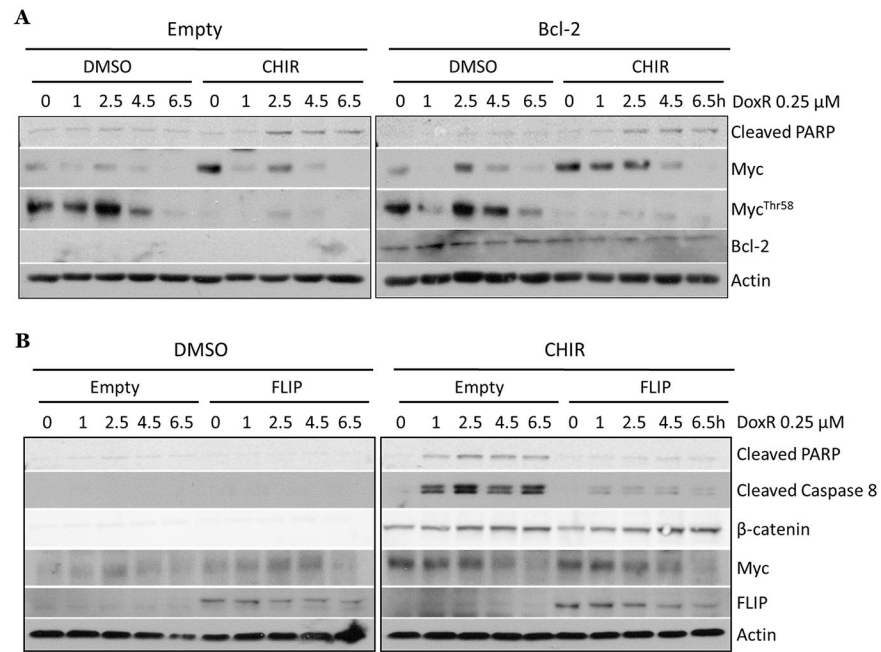


**Figure 6. Disrupting the extrinsic apoptotic pathway abrogates the pro-apoptotic effects of anti-GSK-3 $\beta$  adjuvant therapy.**

**A)** Ramos cells expressing an empty vector construct or the Bcl-2 construct were treated for 2 hours with DMSO or 3  $\mu$ M CHIR99021 followed by a 6.5 hour time course of .25  $\mu$ M doxorubicin. Western blotting was performed for Myc, Myc<sup>Thr58</sup> phosphorylation, cleaved PARP, and Bcl-2. **B)** Ramos cells expressing an empty vector construct or FLIP construct were treated as in A). Western blotting was performed for markers of GSK3- $\beta$  inhibition, cell death, and FLIP expression.

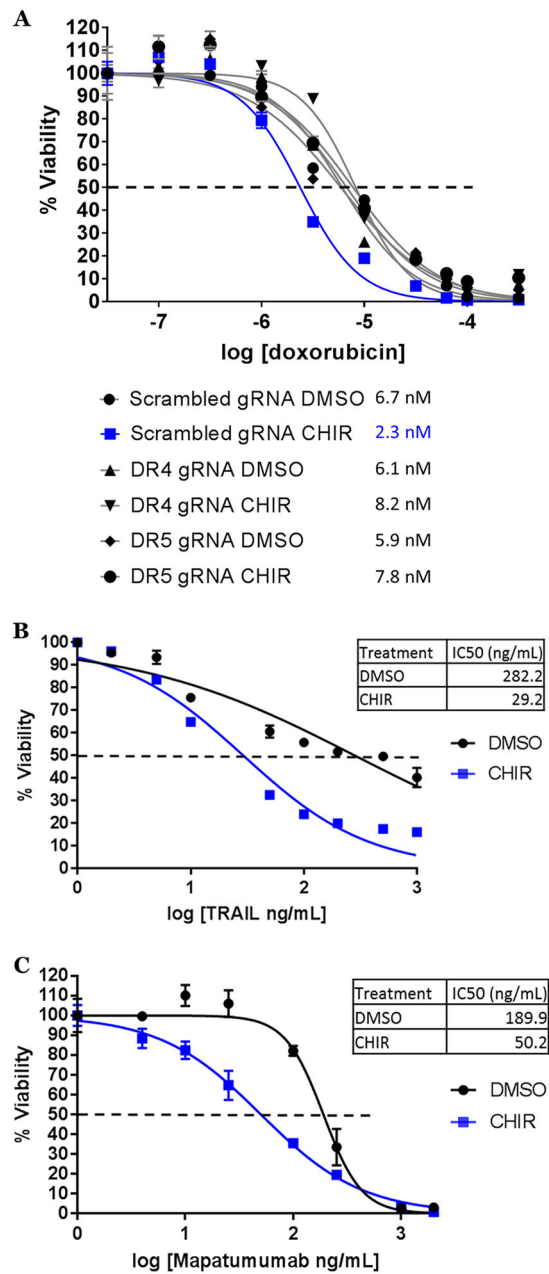


**Figure 7. Anti-GSK-3 $\beta$  adjuvant therapy engages and relies on the extrinsic apoptotic pathway.** A) Ramos derivative cell lines with scrambled gRNA, DR4 gRNA, and DR5 gRNA were treated and cell survival assessed as in Fig. 2C. B) and C) Ramos cells were treated with DMSO or 3  $\mu$ M CHIR99021 and increasing concentrations of TRAIL (B) or mapatumumab (C) for 72 hours and analyzed as in A).

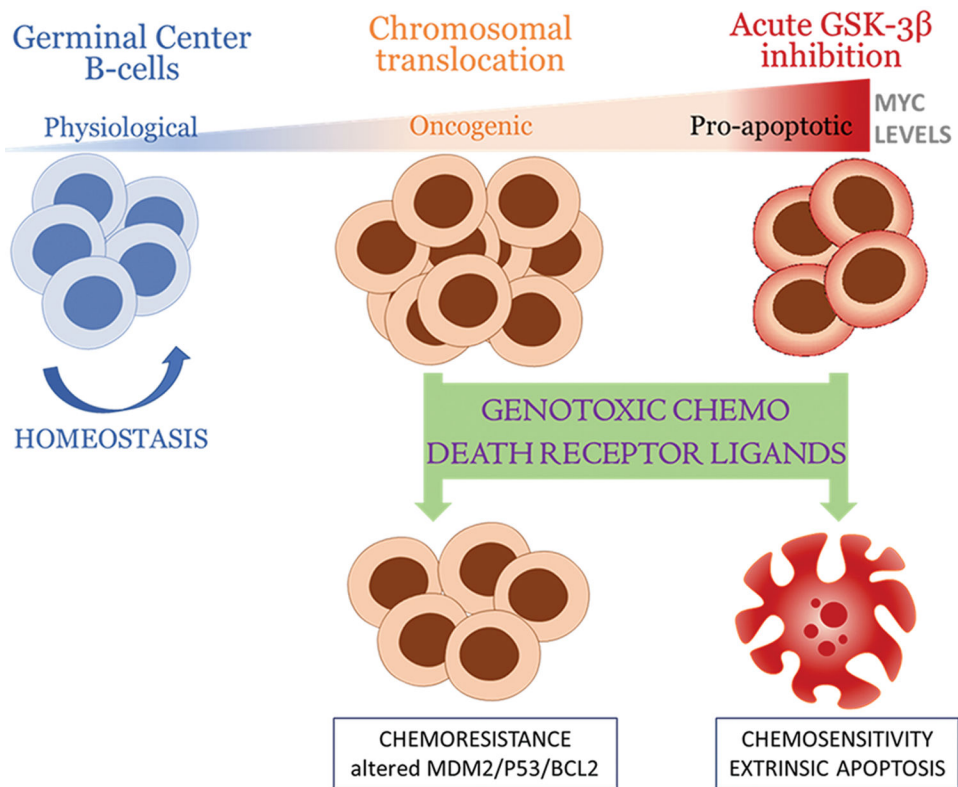


**Figure 8.** Model of sensitization of B-cell lymphomas to therapeutic agents by GSK-3 $\beta$  inhibition and stabilization of Myc.